Electronic Supplementary Material (ESI) for RSC Advances.
This journal is © The Royal Society of Chemistry 2021

Supporting Information

Study on the Enhancing Water Collection Efficiency of Cactus- and Beetle-like Biomimetic Structure Using UV-induced Controllable Diffusion Method and 3D Printing Technology

*Linhui Peng, †, ‡ Keqiu Chen, †, ‡ deyi Chen, † Jingzhi Chen, † Jie Tang, † Shijie Xiang, † Weijiang Chen, †Pengyi Liu, *, † Feipeng Zheng, *, † and Jifu Shi*, †*

†Siyuan Laboratory, Guangzhou Key Laboratory of Vacuum Coating Technologies and New Energy Materials, Department of Physics, Jinan University, Guangzhou 510632, China.

‡These authors contributed equally.

Corresponding Author

* E-mail: tlpy@jnu.edu.cn.

* E-mail: fpzheng_phy@email.jnu.edu.cn.

* E-mail: shijifu2017@126.com.

Contents

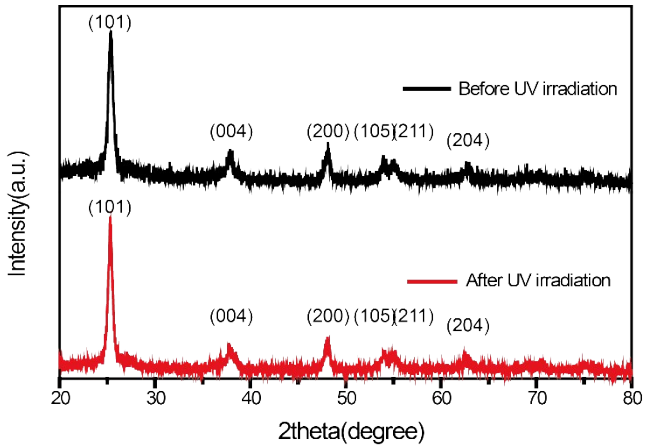

Figure S1 XRD pattern of the sample before (black curve) and after (red curve) UV irradiation. It could be seen that anatase-phase titanium dioxide are both detected before and after UV irradiation. (JCPDS card no. 21-1272)

a

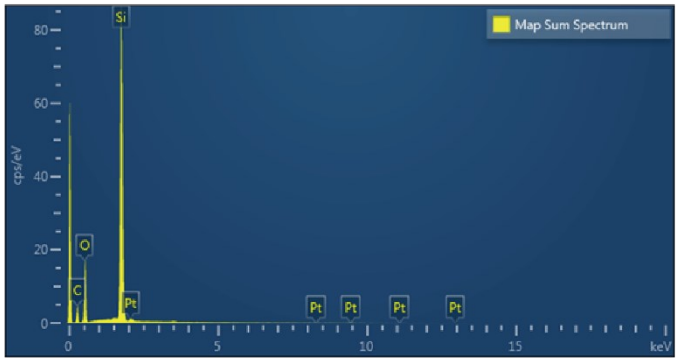

Element	Atomic%
C	39.3
O	33.1
Si	27.6
total	100

b

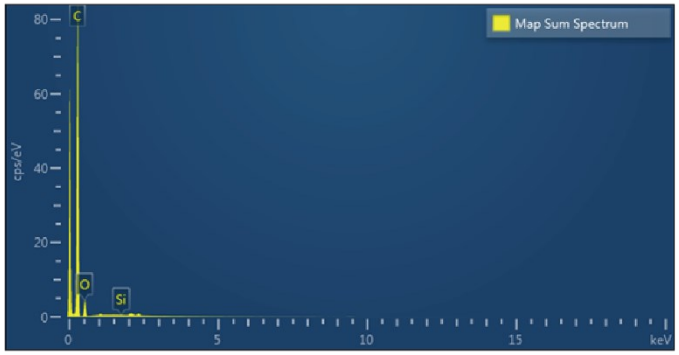

Element	Atomic%
C	88.1
O	11.9
Si	0
total	100

Figure S2 Energy dispersive spectroscopy (EDS) analysis on componential elements proportion of the (a)HB adhesive, (b)HL adhesive. This indicates that Si element only exists in the HB adhesive, so Si element is the characteristic owned by HB adhesive.

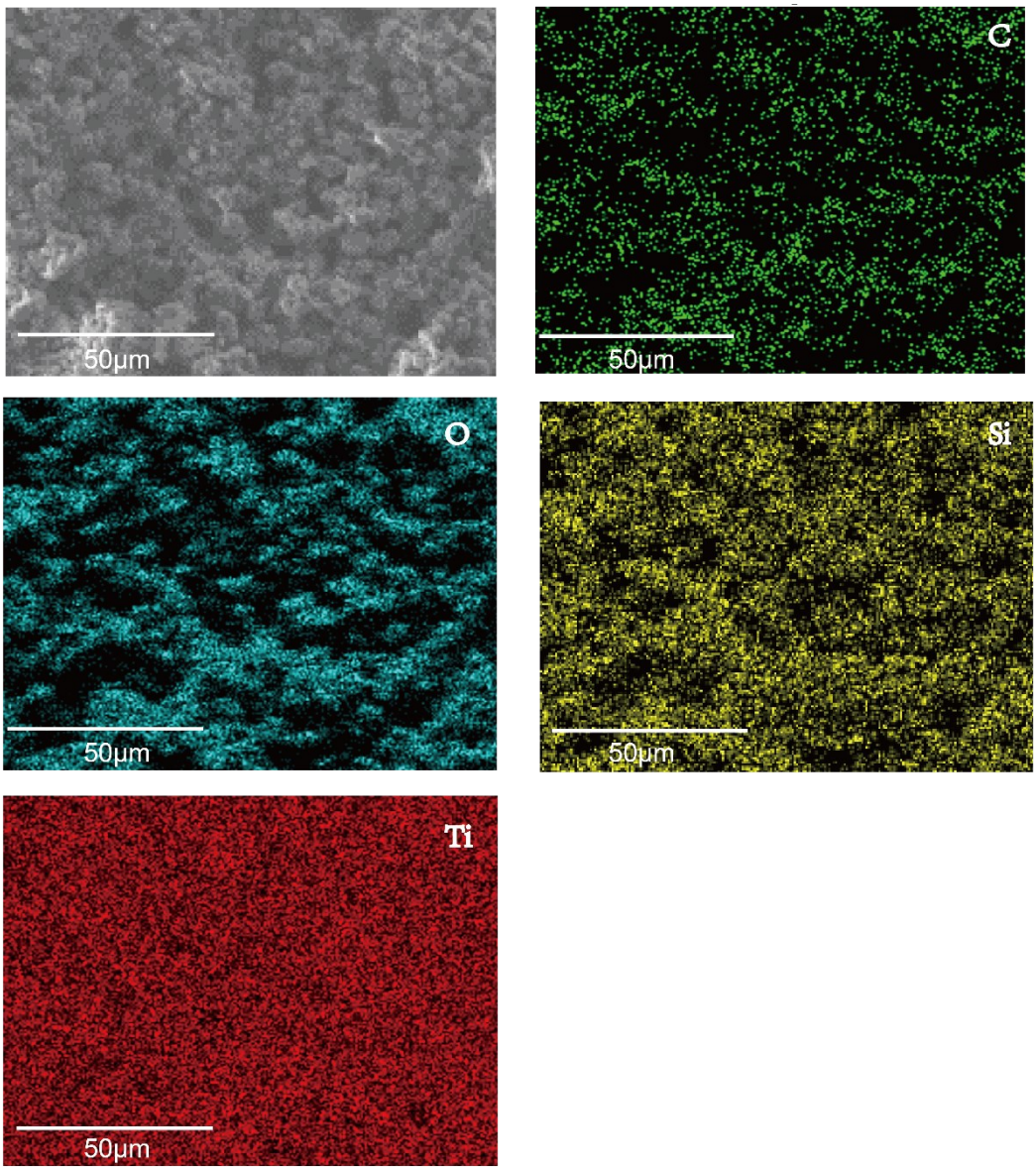

Figure S3 SEM images via energy dispersive spectroscopy (EDS) analysis on elements distribution of HB-HL-TiO_2 sample after UV irradiation. For the whole system, C, O, Si and Ti element indicated with green, blue, yellow and red colors. This indicate that we can assess the distribution of superhydrophobic region on the hybrid wettability surface via Si element distribution (the mass ratio of hydrophobic and hydrophilic adhesives is 1:1 and the UV irradiation time is 2h).

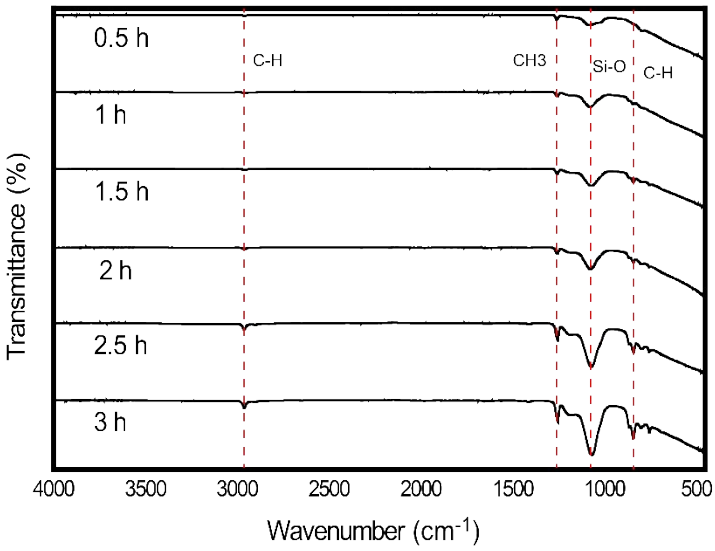

Figure S4 FTIR of the sample with different UV irradiation time. It could be seen that the intensity of characteristic peaks centered at 2959.7, 1252.5, 1076.5 and 814.8 cm^{-1}, corresponding to the stretching vibrations of C-H, CH_3, Si-O and bending vibration of C-H of the organosilicon adhesive, increase gradually as the UV irradiation time increases. This result indicates that the longer the UV irradiation time is, the more the small molecules owned by organosilicon diffuse upward, leading to more superhydrophobic region (the sample with 1:1 ratio of HB-HL adhesive).

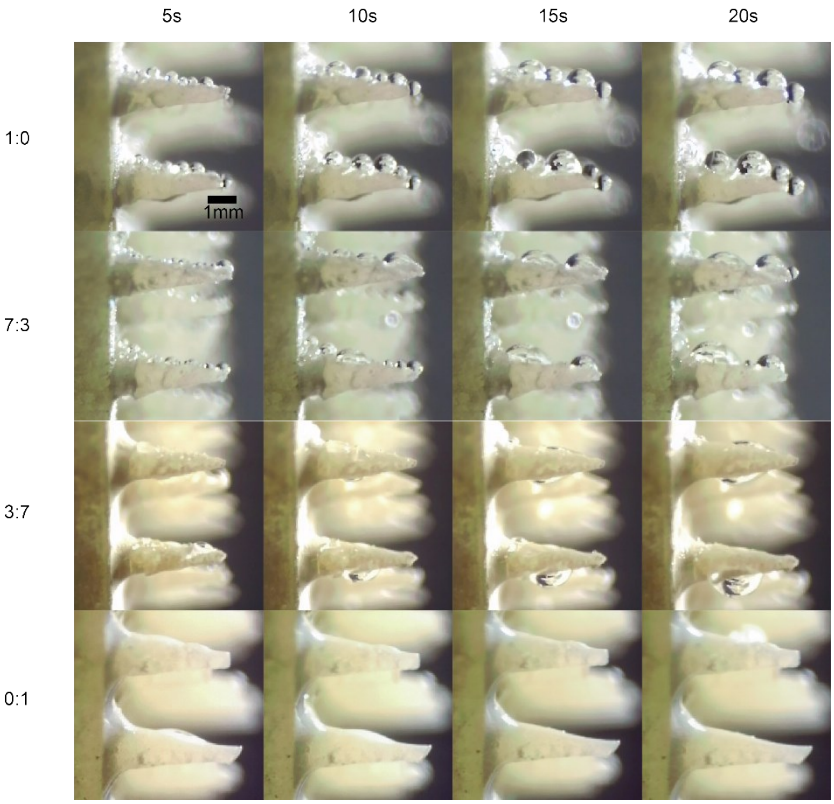

.

Figure S5 Side view of photographs of the samples magnified around specific cones at the times of 5, 10, 15 and 20 s for the sample with the mass ratios of hydrophobic and hydrophilic adhesives 1:0, 7:3, 3:7 and 0:1.

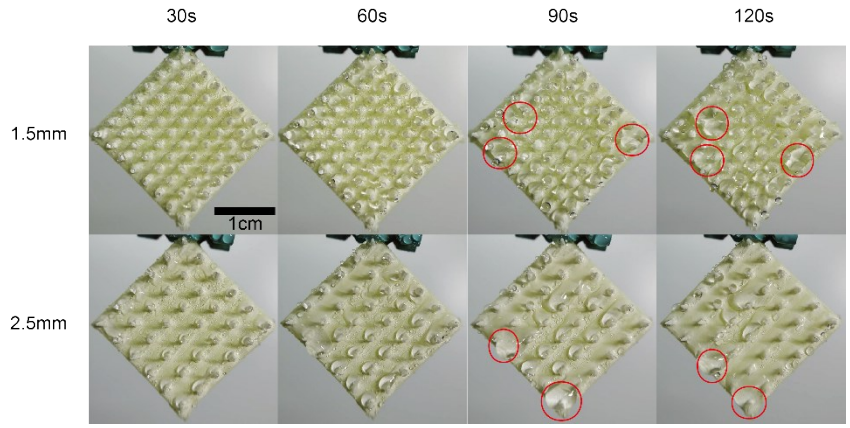

Figure S6 The same as Figure 6c in the main text, but with different cone distances, which are 1.5 and 2.5 mm, respectively, in this figure.

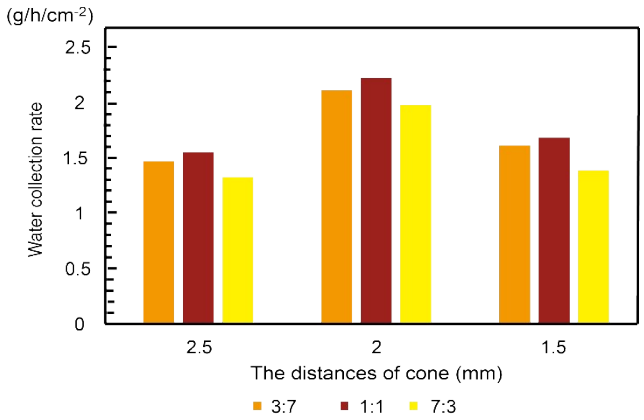

Figure S7 Water collecting rates of the samples with different HB-HL adhesives ratios (3:7, 1:1 and 7:3) and cone distances (1.5, 2.0 and 2.5 mm).

Since the optimal ratios for different structure parameters are all around 1:1, we explore the ratio around 1:1 to confirm the optimal ratio for the samples with different cone distances. Via the control variable method, we measure the water collection rate with respect to the HB and HL ratio for the samples with different cone distances. We found that 1:1 ratio is still the optimal.

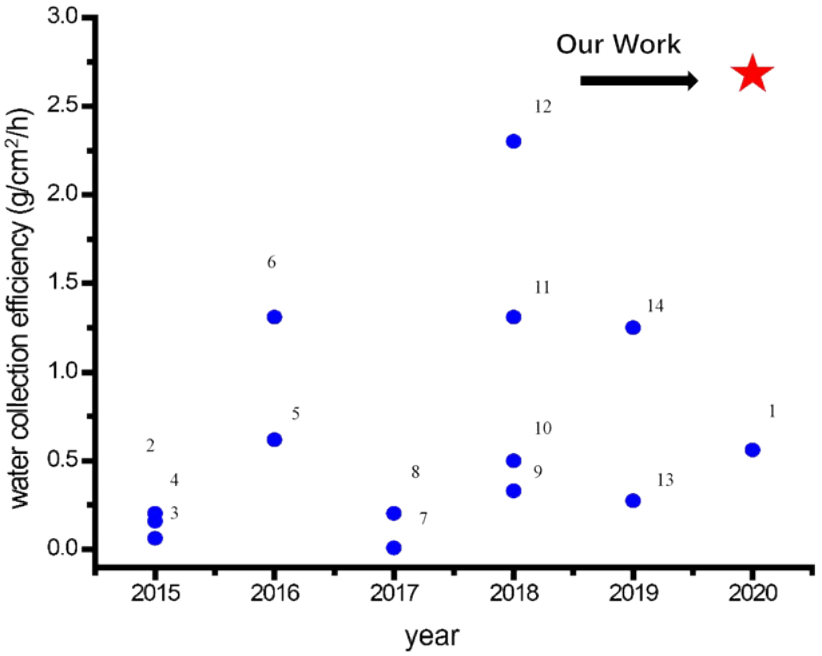

Figure S8 The fog-collecting efficiency of the single biomimetic structure in recent years, which are reported by the references [1-14]. The red star indicates the fog-collecting efficiency of the combining biomimetic structure in this work, which is higher than the single biomimetic structures.

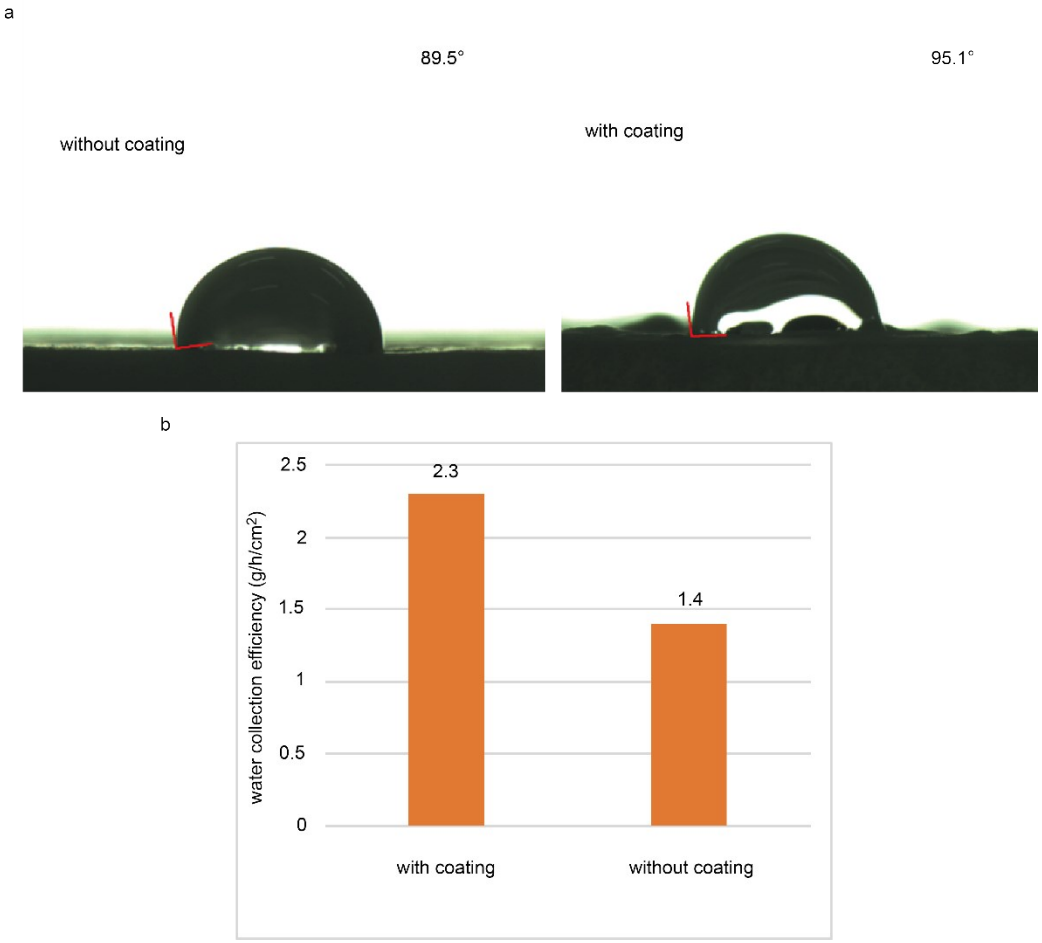

Figure S9 (a) The water contact angle of the sample without coating (left) and with coating (right). The coating consists of hybrid HB-HL adhesives with the mixing ratio of 2:8. (b) The water collection efficiency of the samples with and without coating as described in (a). This shows that the water contact angle of the pristine sample and the hybrid HB-HL structure is close, but the water collection efficiency of the hybrid HB-HL structure is much higher than that of the pristine sample, indicating that the improvement of the water collection capability of the cone arrays is attributed to the hybrid HB-HL structures.

Table S1 The atomic proportion of the HB-HL-TiO_2 sample before and after UV irradiation and the samples (HL-TiO_2, HB-HL-TiO_2 and HB-TiO_2) after UV irradiation measured by XPS. Si and Ti elements are owned by organosilicon adhesive and titanium dioxide, respectively (the ratio of HB-HL adhesive is 1:1 for the HB-HL-TiO_2 sample).

Name	**Atomic % (HB-HL-TiO_2) Before UV**	**Atomic % (HB-HL-TiO_2) After UV**	**Atomic % (HL-TiO_2) After UV**	**Atomic % (HB-TiO_2) After UV**
C 1s	18.6	5.6	20.7	32.2
O 1s	54.2	64.9	53.6	38.8
Ti 2p	26.2	9.9	25.7	2.7
Si 2p	0.5	19.6	0	26.3
Total	100	100	100	100

Table S2 The masses of the first 10 dripping droplet for the perforated and non-perforated samples, respectively.

drop	**Weight (g)** **(Perforated sample)**	**Weight (g)** **(Non-perforated sample)**
1 st	0.044	0.057
2 nd	0.038	0.056
3 rd	0.066	0.042
4 th	0.038	0.036
5 th	0.037	0.038
6 th	0.04	0.067
7 th	0.032	0.067
8 th	0.039	0.041
9 th	0.039	0.038
10 th	0.041	0.035
Average	0.0414	0.0477

Table S3 The water collection rate of the perforated and non-perforated samples.

	WCR (g/h) **(Perforated sample)**	**WCR (g/h)** **(Non-perforated sample)**
1 st	3.281	3.089
2 nd	3.259	3.018
3 rd	3.602	3.048
Average	3.381	3.051

Table S4 The water contact angle of TiO_2 coating in several days after UV irradiation. This indicates the TiO_2 coating can remain superhydrophilicity for a long time after UV irradiation

day	**0**	**1**	**2**	**3**	**4**	**5**	**6**	**7**	**8**	**9**	**10**	**11**	**12**	**13**	**14**	**15**
Water contact angle	0°	0°	0°	0°	0°	0°	0°	0°	0°	0°	0°	0°	0°	0°	0°	0°

Reference:

(1) Wang, J.; Yi, S.; Yang, Z.; Chen, Y.; Jiang, L.; Wong, C. P. Laser Direct Structuring of Bioinspired Spine with Backward Microbarbs and Hierarchical Microchannels for Ultrafast Water Transport and Efficient Fog Harvesting. *ACS Appl. Mater. Interfaces* **2020**, *12* (18), 21080–21087. https://doi.org/10.1021/acsami.0c02888.

(2) Peng, Y.; He, Y.; Yang, S.; Ben, S.; Cao, M.; Li, K.; Liu, K.; Jiang, L. Magnetically Induced Fog Harvesting via Flexible Conical Arrays. *Adv. Funct. Mater.* **2015**, *25* (37), 5967–5971. https://doi.org/10.1002/adfm.201502745.

(3) Zhang, L.; Wu, J.; Hedhili, M. N.; Yang, X.; Wang, P. Inkjet Printing for Direct Micropatterning of a Superhydrophobic Surface: Toward Biomimetic Fog Harvesting Surfaces. *J. Mater. Chem. A* **2015**, *3* (6), 2844–2852. https://doi.org/10.1039/c4ta05862c.

(4) Wang, Y.; Zhang, L.; Wu, J.; Hedhili, M. N.; Wang, P. A Facile Strategy for the Fabrication of a Bioinspired Hydrophilic-Superhydrophobic Patterned Surface for Highly Efficient Fog-Harvesting. *J. Mater. Chem. A* **2015**, *3* (37), 18963–18969. https://doi.org/10.1039/c5ta04930j.

(5) Zhu, H.; Guo, Z. Hybrid Engineered Materials with High Water-Collecting Efficiency Inspired by Namib Desert Beetles. *Chem. Commun.* **2016**, *52* (41), 6809–6812. https://doi.org/10.1039/c6cc01894g.

(6) Xu, T.; Lin, Y.; Zhang, M.; Shi, W.; Zheng, Y. High-Efficiency Fog Collector: Water Unidirectional Transport on Heterogeneous Rough Conical Wires. *ACS Nano* **2016**, *10* (12), 10681–10688. https://doi.org/10.1021/acsnano.6b05595.

(7) Al-Khayat, O.; Hong, J. K.; Beck, D. M.; Minett, A. I.; Neto, C. Patterned Polymer Coatings Increase the Efficiency of Dew Harvesting. *ACS Appl. Mater. Interfaces* **2017**, *9* (15), 13676–13684. https://doi.org/10.1021/acsami.6b16248.

(8) Duan, J.-A.; Du, H.; He, J.; Yin, K.; Wang, C.; Dong, X. A Simple Way to Achieve Bioinspired Hybrid Wettability Surface with Micro/Nanopatterns for Efficient Fog Collection. *Nanoscale* **2017**, *9* (38), 14620–14626. https://doi.org/10.1039/c7nr05683d.

(9) Zhu, H.; Duan, R.; Wang, X.; Yang, J.; Wang, J.; Huang, Y.; Xia, F. Prewetting Dichloromethane Induced Aqueous Solution Adhered on Cassie Superhydrophobic Substrates to Fabricate Efficient Fog-Harvesting Materials Inspired by Namib Desert Beetles and Mussels. *Nanoscale* **2018**, *10* (27), 13045–13054. https://doi.org/10.1039/c8nr03277g.

(10) Yang, S.; Sun, N.; Dai, X.; Nielsen, S. O.; Stogin, B. B.; Wong, T.-S.; Wang, J. Hydrophilic Directional Slippery Rough Surfaces for Water Harvesting. *Sci. Adv.* **2018**, *4* (3), eaaq0919. https://doi.org/10.1126/sciadv.aaq0919.

(11) Zhou, H.; Zhang, M.; Li, C.; Gao, C.; Zheng, Y. Excellent Fog-Droplets Collector via Integrative Janus Membrane and Conical Spine with Micro/Nanostructures. *Small* **2018**, *14* (27), 1–7. https://doi.org/10.1002/smll.201801335.

(12) Bai, H.; Zhang, C.; Long, Z.; Geng, H.; Ba, T.; Fan, Y.; Yu, C.; Li, K.; Cao, M.; Jiang, L. A Hierarchical Hydrophilic/Hydrophobic Cooperative Fog Collector Possessing Self-Pumped Droplet Delivering Ability. *J. Mater. Chem. A* **2018**, *6* (42), 20966–20972. https://doi.org/10.1039/C8TA08267G.

(13) Wang, X.; Zeng, J.; Yu, X.; Zhang, Y. Superamphiphobic Coatings with Polymer-Wrapped

Particles: Enhancing Water Harvesting. *J. Mater. Chem. A* **2019**, *7* (10), 5426–5433. https://doi.org/10.1039/c8ta12372a.

(14) Zhong, L.; Feng, J.; Guo, Z. An Alternating Nanoscale (Hydrophilic-Hydrophobic)/Hydrophilic Janus Cooperative Copper Mesh Fabricated by a Simple Liquidus Modification for Efficient Fog Harvesting. *J. Mater. Chem. A* **2019**, *7* (14), 8405–8413. https://doi.org/10.1039/c9ta01906e.